Metabolic reprogramming in 3D ex-vivo lung adenocarcinoma cancer models

Suehelay Acevedo Acevedo[1], Hayley D. Ackerman[1], Vanessa Y. Rubio[1], Nicole Hackel[1], Kaitlyn A. Miranda[1], Christina Carr[1], Jaden Baldwin[1], Michelle Reiser[1], John Lockhart[1], Paul Stewart[3], Xiaoqing Yu[3], Gina Nazario[4], Hilal Ozakinci[4], John Koomen[1], Duy T. Nguyen[5], W. Gregory Sawyer[5], Gina DeNicola[6], Theresa Boyle[4], Eric Haura[7], and Elsa R. Flores [1,2,+].*

[1]Department of Molecular Oncology, [2]Cancer Biology and Evolution Program, [3]Department of Bioengineering, [4]Department of Pathology, [5]Department of Thoracic Oncology, [6]Department of Cancer Physiology
H. Lee Moffitt Cancer Center and Research Institute, Tampa Florida

MOFFITT CANCER CENTER

BACKGROUND

- Lung adenocarcinoma (LuAD) remains the most diagnosed lung cancer in the United States.
- TP53 (p53) mutations occur frequently in many types of cancer, including LuAD, and are associated with poor prognosis.
- While p53 reactivation failed clinically, alternative strategies have been pursued, including studying and targeting its family members, p63 and p73.
- 3D *ex vivo* models that recapitulate the *in vivo* lung tumor biology, including the microenvironment, are essential to study and validate mechanistic targets of LuAD progression under different p53 statuses (i.e., wild-type [WT], p53 loss, and p53 R172H mutations).

METHODS

LuAD mouse models

Genotype
$Kras^{G12D/+}$
$Kras^{G12D/+}$, $Trp53^{R172H/+}$
$Kras^{G12D/+}$, $Trp53^{\Delta/\Delta}$
$Kras^{G12D/+}$, $TAp73^{\Delta td/\Delta td}$

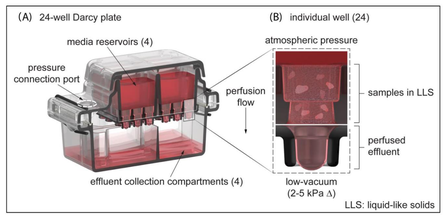

Figure 1 Left: Summary of mouse models used in this study. Schematic of a 24-well Darcy perfusion plate (**A**) depicting a detailed cross-section of an individual well (**B**). As described in Nguyen D. et al. Cells 2022.

Table 1 Summary of patient samples successfully cultured as microtumors.

Tumor type	Tissue Source	Successful Cultures
Lung Adenocarcinoma	OR	4
Lung squamous	OR	1
Lung adenocarcinoma	RTD	6
LuAD Liver metastasis	RTD	3
Small cell lung cancer	RTD	4
SCLC liver metastasis	RTD	1
SCLC brain metastasis	RTD	1

RESULTS

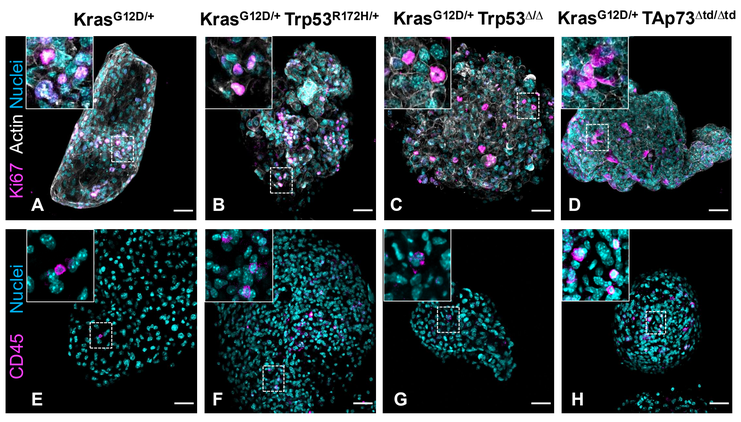

Figure 2 A-D: Representative immunofluorescence images of mouse microtumors stained for Ki67. Actin was stained with phalloidin (white) and nuclei with Hoechst 33342 (cyan). **E-H**: Representative CD45 (magenta) immunofluorescence images of lung adenocarcinoma microtumors derived from mice. Scale bar = 50 µm.

CONCLUSIONS

- Successfully established LuAD microtumors from mouse models that are proliferative for up to 10 days.
- LuAD microtumors retain the endogenous immune microenvironment.
- LuAD microtumors have increased epithelial-to-mesenchymal transition (EMT) signatures at the RNA and protein level.
- Microtumors show lipid reprogramming associated with tumor progression.
- Successfully established *ex-vivo* microtumor cultures of patient LuAD from operating room and Rapid Tissue Donation samples.

RESULTS

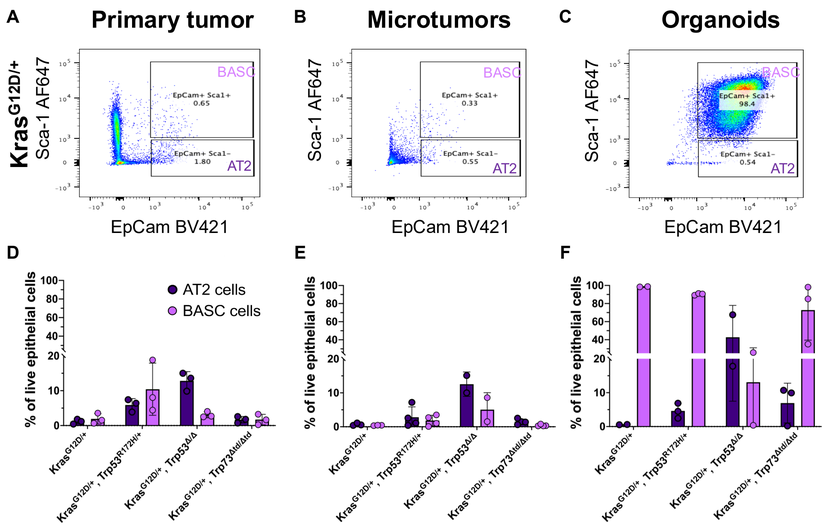

Figure 3 A-C: Representative flow cytometry dot plots of EpCam and Sca1 markers for primary tumor, microtumors, and organoids for the K mouse model. **D-F**: Quantification of AT2 and BASC cell populations in primary tumors, microtumors, and organoid models. N = 3-4 mice per condition. Data shown as mean ± SD.

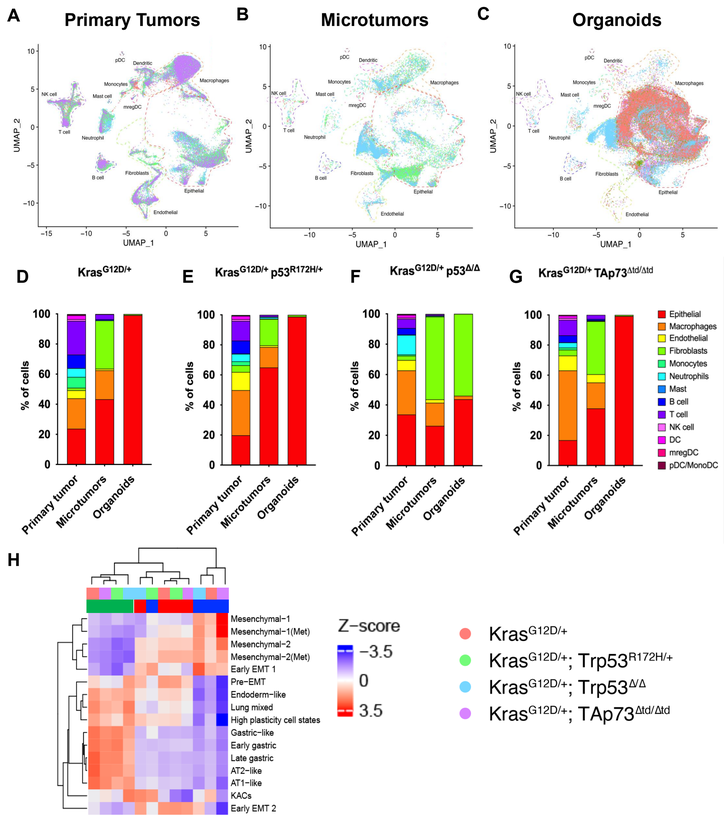

Figure 4 A – C: UMAPs of primary tumors, microtumors, and organoids for all mouse models obtained from single-cell RNA sequencing. **D – G:** Proportion of major cell types for all genotypes. Cell types are described in the legend above. **H:** Heatmap showing the z-scores of various gene signatures in malignant epithelial cells for the primary tumor, microtumors, and organoids for all genotypes. N = 1 – 4 mice per model per genotype.

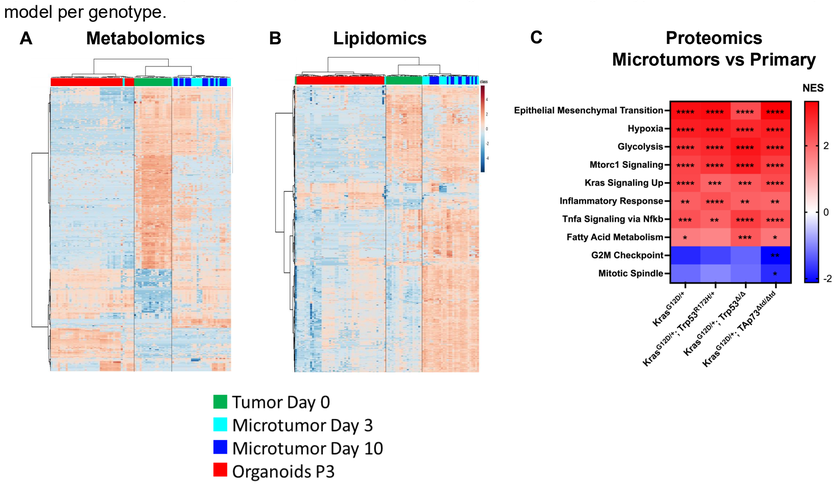

Figure 5 Global metabolomics **(A)** and lipidomics **(B)** heatmaps of primary tumor, microtumor, and organoid tissues. **C:** Heatmap showing the top proteomic pathways in microtumors compared to primary tumors for all genotypes. Colors indicate the normalized enrichment score (NES). *p<0.05; **p<0.005; ***p<0.0005; ****p<0.0001

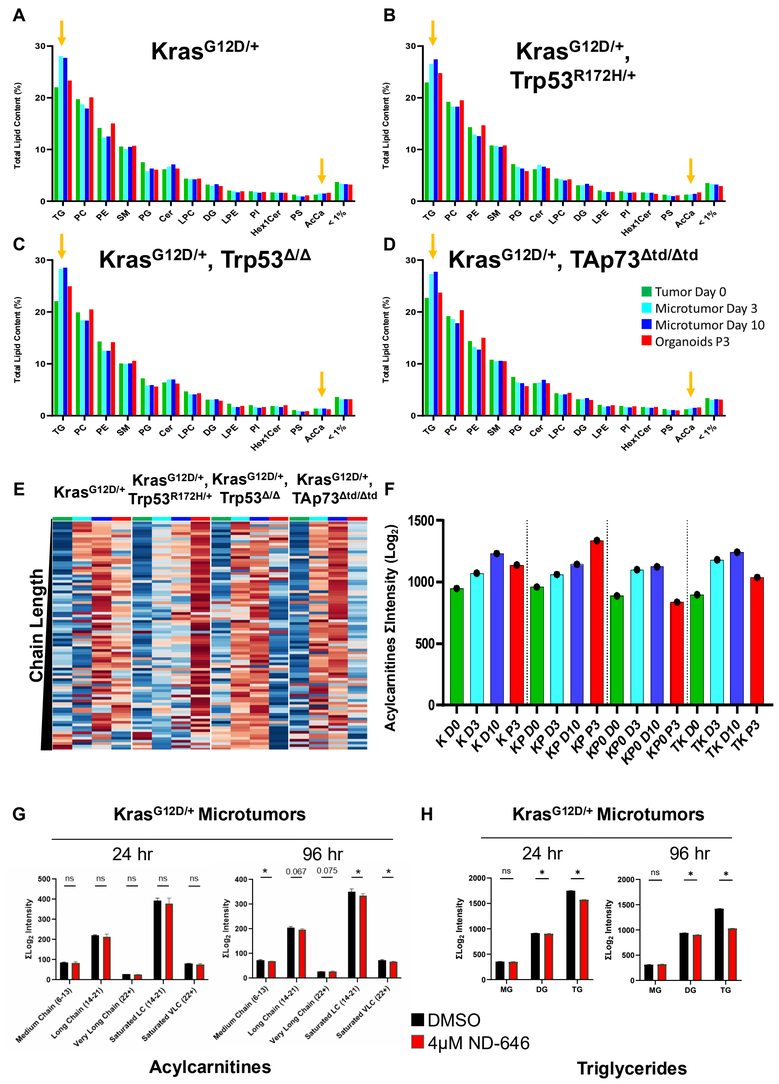

Figure 6 A-D: Percentage of lipid classes for all genotypes. Heatmap (**E**) and quantification (**F**) of acylcarnitine lipid class in primary, microtumor, and organoid models. **G:** Levels of unsaturated and saturated acylcarnitines in $Kras^{G12D/+}$ microtumors treated with the ACC1/2 inhibitor, ND-646. **H:** Levels of triglycerides in $Kras^{G12D/+}$ microtumors treated with ND-646. *p<0.05 N = 2 – 4 samples per treatment.

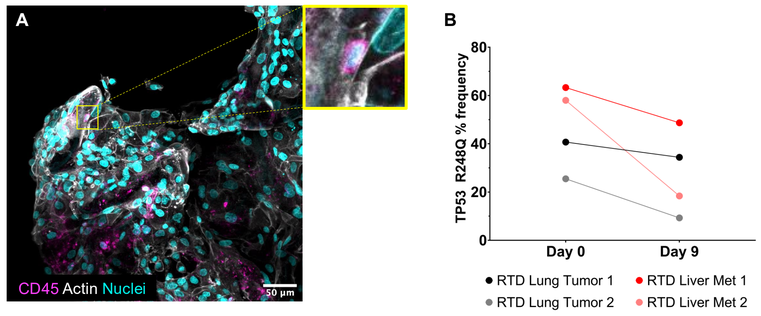

Figure 7 A: Representative CD45 (magenta) immunofluorescence image of a lung adenocarcinoma patient microtumor. Actin was stained with phalloidin (white) and nuclei with Hoechst 33342 (cyan). Scale bar = 50 µm. **B:** STAR testing of TP53 mutation in the primary and metastatic patient tumors and microtumors.

FUTURE DIRECTIONS

- Test if patient microtumors also rely on fatty acid synthesis and exhibit increased acylcarnitines.

ACKNOWLEDGEMENTS

- R35 CA197452
- P01 CA250984
- Rapid Tissue Donation Program
- Moffitt Shared Resources
  - Molecular Genomics Core
  - Proteomics Core
- P01 Cores:
  - Metabolism Core
  - Pre-clinical Core
  - Data Science Core

NIH NATIONAL CANCER INSTITUTE